The Basal Detectability of an Ice-Covered Mars by MARSIS

C. Grima, J. Mouginot, W. Kofman, A. Hérique, P. Beck

▶ **To cite this version:**

HAL Id: insu-03705391
https://insu.hal.science/insu-03705391

Submitted on 19 Aug 2022

AGU
ADVANCING
EARTH AND
SPACE SCIENCE

Geophysical Research Letters®

Correspondence to:

C. Grima,
cyril.grima@utexas.edu

The Basal Detectability of an Ice-Covered Mars by MARSIS

C. Grima[1] , J. Mouginot[2] , W. Kofman[3,4] , A. Hérique[3] , and P. Beck[3]

[1]Institute for Geophysics, The University of Texas at Austin, Austin, TX, USA, [2]University Grenoble Alpes, CNRS, IGE, Grenoble, France, [3]University Grenoble Alpes, CNRS, CNES, IPAG, Grenoble, France, [4]Centrum Badan Kosmicznych Polskiej Akademii Nauk (CBK PAN), Warsaw, Poland

Abstract The detection of anomalously strong relative basal reflectivity beneath the Martian South Polar Layered Deposits (SPLD) from the Mars Advanced Radar for Subsurface and Ionosphere Sounding (MARSIS) has led to hypotheses suggesting the presence of basal materials such as liquid water. Here, we propose a forward approach to assess whether such a high signal could be produced by a Martian terrain currently exposed at the surface without liquid water. We convert existing MARSIS surface reflectivity measurements into a basal reflectivity as if it were overlaid by an SPLD-like ice deposit. 0.3%–2% of the surface could produce basal reflections of magnitude similar to the SPLD measurements in the assumption of a 10% impure ice. An ice loss tangent >0.01 is required to prevent any of the current Martian surface from producing a bright SPLD-like basal reflection. The detected bright terrains are gathered within volcanic constructs of diverse geologic epoch.

Plain Language Summary The presence of stable liquid water on Mars might provide an environment appropriate for the sustainability of extraterrestrial life. However, the current temperature and pressure at the Red Planet makes stable liquid water unlikely at the surface. A debate has emerged over the recent years from the detection of an anomalously bright radar return from the base of the South polar cap, down to 1.4 km deep beneath the ice. Early interpretations have proposed this signal to originate from water-bearing material, or even subglacial lakes. This is being disputed by laboratory measurements suggesting clay, metallic inclusions or saline ice as alternative materials. Here, we aim to determine if Martian terrains today could produce strong basal echoes if they were covered by a planet-wide ice sheet. The strength of this approach is to rely on already measured radar reflection properties of the surface across the whole planet. We find that some existing volcanic-related terrains could produce a very strong basal signal analog to what is observed at the South polar cap. Our analysis strengthens the case against a unique hypothesis based solely on liquid water for the nature of the polar basal material.

1. Introduction

Anomalously bright basal reflections have been detected at the South Polar Layered Deposits (SPLD) of Mars by the Mars Advanced Radar for Subsurface and Ionosphere Sounding (MARSIS) onboard the Mars Express spacecraft (Lauro et al., 2020; Orosei et al., 2018). Bright radar returns are typically produced by materials of high permittivity, leading to the initial interpretation that liquid water could be present at the base of the SPLD, whether in a water bearing material or through a coherent water body (Lauro et al., 2020; Orosei et al., 2018, 2020). Orosei et al. (2018) used the assumption of a non-conductive material to invert the basal relative permittivity from reflectivity measurements. They found that the permittivity to be in the range of 4–15 outside the bright area, which is a conservative range encompassing most of the sedimentary and igneous rocks that could be encountered on Mars or Earth (Campbell & Ulrichs, 1969; Telford et al., 1990). In contrast, this number for the bright area inside the SPLD is deduced to be >15 with a median at 33 when accounting for various assumptions for the overlying ice properties Orosei et al. (2018).

Basal liquid water is thought to be hardly sustainable at the present-day Martian geothermal conditions, even with a large amount of salts that would depress the ice melting point (Sori & Bramson, 2019). Only local heat anomaly could ultimately melt the ice (Arnold et al., 2019; Sori & Bramson, 2019), but bright basal radar returns appear to be ubiquitous through the SPLD by contrast with the spatially confined early detection (Khuller & Plaut, 2021). Alternative basal composition that do not necessarily require liquid water have been proposed to produce such strong radar returns. By contrast with the assumption in Orosei et al. (2018), most rely on conductive materials such as clay, metal-bearing minerals, or saline ice (Bierson et al., 2021; Smith et al., 2021; Tulaczyk & Foley, 2020). However high electrical conductivity contrasts are not the only possibility, a structural setting

from alternations of thin layers of H_2O, CO_2 or possibly pure smectite, at the surface and/or the base of the SPLD could produce bright echoes through constructive interference of the radar signal (Lalich et al., 2021; Mouginot et al., 2009; Smith et al., 2021).

The main metric that has been used to assess the reflective strength of the SPLD/bedrock interface is the relative basal reflectivity defined as the power ratio of the subsurface echo against the surface echo P_{ss}/P_s (Lauro et al., 2010). At the location where the bright radar return is, P_{ss}/P_s at 4 MHz is consistently measured higher than 0 dB with a median at about 2.5 dB. It exhibits excursions above 5 dB but rarely exceeds 10 dB (Lauro et al., 2020; Orosei et al., 2018, 2020). Under the assumption of a 205 K SPLD ice with 10% dust content, Orosei et al. (2018) have discussed that a $P_{ss}/P_s > 0$ dB corresponds to a basal permittivity >15, indicative of the presence of liquid water below polar deposits on Earth (Oswald & Gogineni, 2008; Peters, 2005). The relative basal strength then increases with the liquid water content at the base.

Usually, analytical methods, numerical models, or laboratory/field analogs are used to search for materials that could produce such strong basal reflections (Bierson et al., 2021; Lauro et al., 2020; Smith et al., 2021). However, MARSIS also provides planet-wide surface reflectivity measurements that consequently span the most exhaustive range of terrains that could be geologically produced on the planet, with the acknowledged caveat that their composition is not as well known as laboratory-investigated materials (Mouginot et al., 2010). We propose a forward approach with the aim to infer what would be P_{ss}/P_s if the existing Martian terrains, as measured by MARSIS, were covered by an ice sheet with a thickness similar to the SLPD at the location of the bright basal reflector. We use the surface reflectivity measured by MARSIS to infer the reflection coefficient of today's surface if it was overlaid by an ice deposit. We then derive P_{ss}/P_s values across a range of transmission and attenuation losses to deduce what would be the relative basal reflectivity of a globally ice-covered Mars, and we compare it with the one measured at the SPLD by other authors (Lauro et al., 2020; Orosei et al., 2018). Finally, we use the current assumption that SPLD ice contains 10% of impurities in volume to map what type of Martian terrains could be responsible for a bright basal echo.

2. Data

MARSIS is a multi-frequency radar sounder on board the European Space Agency Mars Express spacecraft (Picardi et al., 2005). Its linear antenna transmits 1-MHz-wide chirped signals centered at 1.8, 3, 4, and 5 MHz. A portion of the radiated power is reflected back to the antenna by each geologic dielectric gradients until signal extinction. The strength, phase, and time delay of each echo is recorded by the radar while empirical measurements demonstrate a penetration depth up to 4 km in the ice of the SPLD (Plaut et al., 2007).

MARSIS is still operating today, providing about 15 years of quasi-uninterrupted measurements. In this study, we use the surface reflectivity data set derived by Mouginot et al. (2010). Arguably, the time series is much more limited than the up-to-date MARSIS data products. However, this is overcome by several assets making it sufficient and suitable for our purpose: (1) It is readily available to the authors without additional data processing; (2) it is corrected from ionospheric distortion (Mouginot et al., 2008; Safaeinili et al., 2007); (3) It already provides a quasi-global coverage of Mars; (4) It is validated for science application through its use in several publications (Mouginot et al., 2009, 2010, 2012).

Mouginot et al. (2010) provide processed surface reflectivity for the 3, 4, and 5 MHz bands. Here, we use exclusively the 4-MHz band as it has the largest spatial coverage. It is also the main frequency used by Orosei et al. (2018) and Lauro et al. (2020) to illustrate and quantify the bright basal reflector at the SPLD. Data are binned into a spatial grid made of $0.5° \times 0.5°$ cells. The median of the linear surface reflectivity power is considered for each cell.

3. Method

A propagation medium can be characterized through its complex permittivity $\varepsilon = \varepsilon' + i\varepsilon''$. The signal attenuation within the medium can be derived from the loss tangent $\tan \delta = \varepsilon''/\varepsilon'$. Our base model considers three propagation media with their own respective permittivity: the Martian atmosphere ($\varepsilon_1 \approx 1$), the ice-sheet material (ε_2), and non-ice sheet materials (ε_3). The cross-section in Figure 1 illustrates the relative emplacement of those
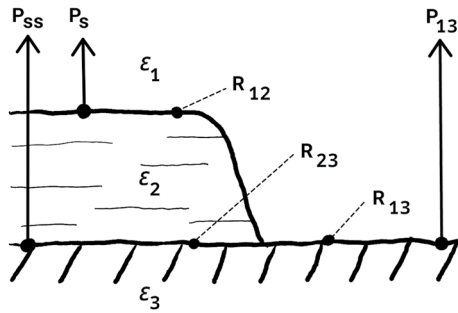
Figure 1. Considered geophysical setting. Subscripts 1, 2, and 3 refer to the atmosphere, the ice, and other terrains, respectively.

media. The signal strength reflected at normal incidence by each interface is described by the reflection coefficient between two non-magnetic media subscripted i and j, respectively, such as:

$$R_{ij} = \left| \frac{\sqrt{\varepsilon_i} - \sqrt{\varepsilon_j}}{\sqrt{\varepsilon_i} + \sqrt{\varepsilon_j}} \right|^2, \quad for \quad \varepsilon_{\{i,j\}} \geq 1 \quad and \quad 0 < R_{ij} < 1 \quad (1)$$

R_{13} defines the surface power reflection coefficient of the various Martian terrains across the planet as provided by Mouginot et al. (2010) from the reduction of the surface echo strength P_{13} recorded at the antenna. If one let Mars be covered by a fictive global ice sheet, the basal reflection coefficient between the existing terrains and the overlying ice would be:

$$R_{23} = \left| \frac{\sqrt{\varepsilon_2} - \sqrt{\varepsilon_3}}{\sqrt{\varepsilon_2} + \sqrt{\varepsilon_3}} \right|^2, \quad for \quad \sqrt{\varepsilon_3} = \frac{1 + \sqrt{R_{13}}}{1 - \sqrt{R_{13}}} \quad (2)$$

It is noteworthy that this expression given for $\sqrt{\varepsilon_3}$ makes the assumption of a quasi non-conductive material (i.e., a dielectric with $\tan \delta \ll 1$) for the geologic terrains making up the Martian surface (Tulaczyk & Foley, 2020) in order to test the hypothesis in Orosei et al. (2018). It is also a convenient assumption in order to produce a simple transfer function between the measured surface reflectivity R_{13} and the hypothetical basal reflectivity R_{23} associated to it. However, by contrast with Orosei et al. (2018), the assumption of non-conductivity is not used here to invert a permittivity from the measured signal strength. Should a material at the surface violate our assumption by being highly conductive, the balance between the real and imaginary part of its permittivity has to vary to accommodate the reflectivity recorded by MARSIS, but the latter does not change as it is an empirical measurement.

Finally, the relative basal reflection coefficient P_{ss}/P_s for a global ice sheet is proportional to the ratio between R_{23} and the surface reflection coefficient of the ice R_{12} (Orosei et al., 2020)

$$\frac{P_{ss}}{P_s} = \frac{R_{23}}{R_{12}} T_{12}^2 A_2 \quad (3)$$

where $T_{12} = 1 - R_{12}$ is the transmission coefficient through the ice surface. The two-way signal attenuation in the ice is given by $A_2 = \exp(-2\pi f\tau \tan \delta_2)$ where f is the radar frequency and τ is the one-way propagation time through the ice.

3.1. Application

Our aim is to calculate P_{ss}/P_s for an ice-covered Mars through Equation 3 by using the observed MARSIS surface reflectivity as a proxy to estimate the basal reflection coefficient R_{23} (Equation 2). To this end, we substitute R_{13} in Equation 2 by $R_{13} = \tilde{R}_{13}R_{12}$. $\tilde{R}_{13}$ is the measured MARSIS surface reflectivity normalized so that a value of unity equals the surface reflectivity at a reference zone above the SPLD bright reflector (discussed in the next paragraph). The losses due to signal propagation in the ice are conveyed into Equation 3 by assumptions on ε_2 and $\tan \delta_2$ that are used to obtain the terms R_{12}, T_{12}, and A_2 thanks to the relationships provided through Section 3.

In our application, we bound the reference zone by 192–194°E and 80–82°S. It is an area of fairly homogeneous surface reflectivity centered on the bright SPLD basal reflections (Lauro et al., 2020). Noteworthily, this area overlaps the reference zone considered by both Mouginot et al. (2010) and Grima et al. (2012) for MARSIS and the Shallow Radar (SHARAD), respectively, for surface reflectivity analysis (180–200°E and 81.5–84.5°S). It accounts for one of the flattest region of Mars with root-mean-square heights <0.3 m at SHARAD wavelength (15 m), ensuring a strongly coherent and specular surface (Grima et al., 2012). Our choice of a reference zone restricted over a tight and bright area is conservative by comparison to other similar studies. For example, Khuller and Plaut (2021) produced a P_{ss}/P_s map from the bed returns measured at the SPLD by considering the average power of the SPLD surface. However, the surface at MARSIS wavelength can produce faint surface returns from superficial CO_2 ice deposits (Lalich et al., 2021; Mouginot et al., 2009) that would contribute to lower the average surface returns across the cap and consequently increase P_{ss}/P_s.
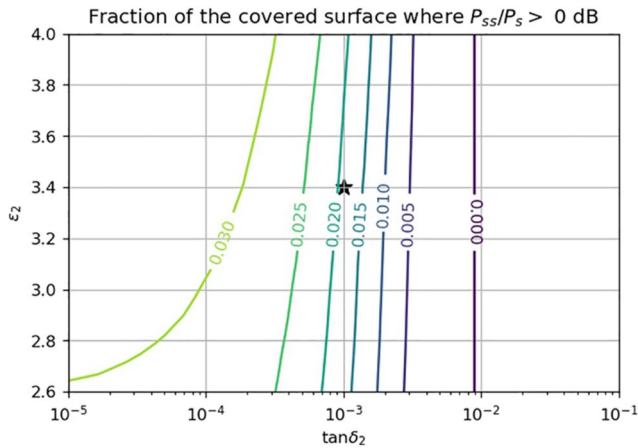
Figure 2. Curves indicating the surface fraction that would produce a relative basal echo strength greater than 0 dB, as a function of ice dielectric properties (ε and $\tan \delta_2$). For ice consistent with SPLD ice (star), about 0.02 of the surface will generate the appropriate reflection coefficient.

P_{ss}/P_s curves resulting from the above methodology are presented in Figure S1 in Supporting Information S1 as a function of $\tilde{R}_{13}$ as well as different $\tan \delta_2$ and for a fixed $\varepsilon_2 = 3.4$. For reference, a map of $\tilde{R}_{13}$, the normalized reflectivity measured by MARSIS at 4 MHz, is provided in Figure S2 in Supporting Information S1. It is highly similar to Figure 5A in Mouginot et al. (2010) since their reference zone overlaps ours.

4. Results

Assuming a relatively homogeneous coverage of Mars by our dataset, the surface fraction that would produce a positive relative basal echo strength is shown in Figure 2 for a range of ice dielectric properties. Solutions exist for $\tan \delta < 0.010$. The SPLD bright basal returns have also been measured with excursions above $P_{ss}/P_s > 5$ dB (Orosei et al., 2018). The corresponding surface fractions for this threshold are shown in Figure S3 in Supporting Information S1.

These results have to be put into perspective with our current knowledge of the electrical properties of the ice at the SPLD. The volumetric impurity rate of the SPLD has been assessed by MARSIS measurements to be about 10% (Plaut et al., 2007; Zuber et al., 2007). This translates to a relative permittivity of $\varepsilon_2 = 3.4$ using the volume mixture model of Looyenga (1965) with an inclusion permittivity of 7 to represent dust of igneous origin (Campbell & Ulrichs, 1969) into a water ice matrix. The corresponding loss tangent at 4 MHz is rather poorly constrained but is estimated to be <0.001–0.005 (Orosei et al., 2020; Plaut et al., 2007). We consider $\tan \delta_2 = 0.001$ as it also matches the theoretical derivation of the loss tangent for a 10%-impure ice (Orosei et al., 2020). As stated before, τ is set to 17 μs to match observations (Lauro et al., 2020; Orosei et al., 2018), which is equivalent to ~1400 m of ice thickness. Under these conditions, about 2% (resp. 0.3%) of the surface would produce a positive (resp. >5 dB) relative basal return P_{ss}/P_s (Figures 2 and S3 in Supporting Information S1), equivalent to the radiometric signature observed for the bright basal reflectors at the SPLD. This makes a reasonable argument for considering current Martian terrains as possible materials responsible for the bright SPLD detection.

We localize those bright terrains by mapping the calculated P_{ss}/P_s using Equation 3 with the ice dielectric properties derived from the 10% volumetric impurity fraction described above. Four insets in Figure 3 highlight some of those regions where a positive P_{ss}/P_s signature is consistent across longitudes instead of just being confined locally along an orbit (an indicator of possible data glitch).

According to the literature summarized below, most of those regions are related to terrains of igneous origin, but all volcanic terrains do not exhibit such a strong signal. Of note, these regions do not share a common geological epoch but are spread over a large timescale from late Noachian to late Amazonian. Their spatial extent is also usually larger than the bright basal area reported by Orosei et al. (2018). The strong basal reflections in Arabia Terra are in a confined spot that is located south of friable-layered deposits related to an ancient highland igneous construct produced by a Noachian-early Hesperian long-lasting volcanic activity (Michalski & Bleacher, 2013; Whelley et al., 2021). Some bright reflections are gathered within Cerberus Palus, a subset unit of the largest Elysium Planitia interpreted to be Amazonian flood basalt plains resulting from some of the most recent Martian volcanic events (Cassanelli & Head, 2018, and references there in). A broad region of strong reflections is identified East of the Uranius Tholus interpreted as a shield volcano resulting from effusive eruptions of low viscosity lavas during the Hesperian-Amazonian transition (Plescia, 2000). The late Hesperian Solis Planum collects bright reflections over the largest area. It is located south-east of the volcanic Tharsis bulge and characterized by wrinkle ridges attesting for horizontal crustal shortening (Montési, 2003).

Whatever material composition is responsible for these bright reflections, it does not have to lie at the very top of the surface since constructive interference from a buried interface can also enhance the MARSIS signal. MARSIS reflectivity is sensitive the vertical slice below the surface, the so called near-surface, that is related to the vertical resolution of the radar. For basaltic-like permittivity, the near-surface approaches 60 m depth (Mouginot et al., 2010).
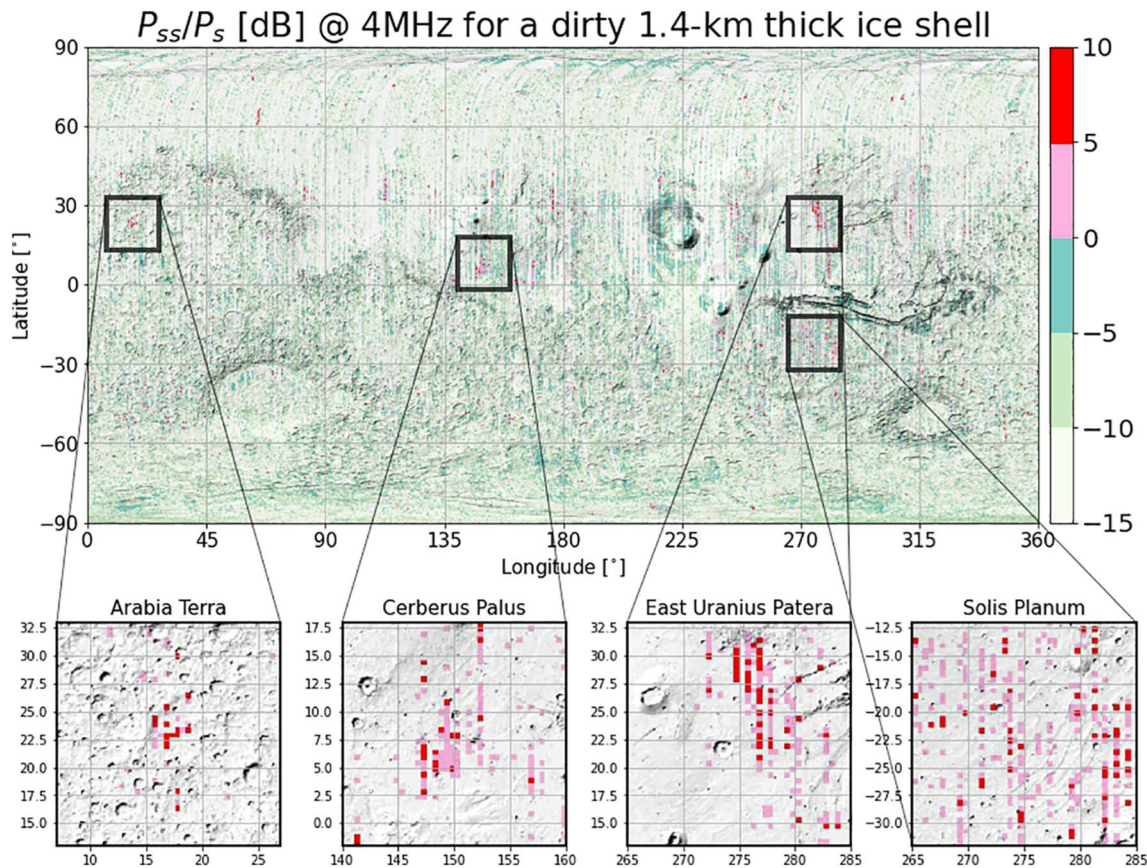
Figure 3. Relative basal echo strength of Mars if the surface was entirely covered by an 1.4-km dirty ice sheet (10% volume impurity rate). Bottom inserts display only positive values for better identifications relative to the regional landforms. The maps are shaded with the Mars Orbiter Laser Altimetry (MOLA) data.

5. Discussions and Conclusions

We proposed and applied a forward approach to assess the relative basal reflection of Mars if it was covered by a global ice sheet. The electric bulk properties of this fictive planetary-wide ice cover are derived from a 10% ice impurity rate (tan $\delta = 0.001$, $\varepsilon_2 = 3.4$), in accordance with current estimates for the ice of SPLD where bright basal reflections have been measured by Orosei et al. (2018) and Lauro et al. (2020). We adopt a conservative approach by not accounting for basal scattering losses due to roughness that would ultimately strengthen the derived relative strength if filtered out from the signal. We acknowledge that the presence of volume scattering, which is not taken into account in this study, would have the opposite effect. Still, those assumptions are identical to what is considered by Orosei et al. (2018), thus providing a common ground for comparing their results at the SPLD with our assessment of the Martian surface capability to produce similar signals. MARSIS recordings synthesize the effect of complex permittivity into a single scalar. As a consequence, our method cannot discriminate on the conductive nature of the observed terrains, but it is still valid to locate what unit at the surface could produce the signal strength reported by Orosei et al. (2018) at the base of the SPLD.

0.3%–2% of the Martian surface could produce reflections analogous to the SPLDs' if covered by ice. The surface rapidly ceases to produce basal reflections similar to the SPLD detection for tan $\delta_2 > 0.010$. It draws attention that the brightest terrains across the planet would produce basal echoes with a radiometric character in the range of the brightest ones observed at the SPLD by Orosei et al. (2018) and under similar assumptions for the composition of the overlying ice. This radiometric similarity (or continuity) is indicative of the likelihood for a non-wet generic material currently available at Mars to be responsible for the bright basal SPLD reflection.

Our results provide insights into what current terrains existing at the surface of Mars could be responsible for the SPLD bright basal reflections. Most of those bright regions are subdivisions of larger units geologically related

to volcanic constructs but not restricted to a specific geologic epoch as they are dated regional studies from the late Noachian to late Amazonian by regional studies.

Orosei et al. (2018) determined permittivity >15 for the bright basal SPLD reflectors with the assumption of negligible conductivity. Because we use similar assumptions for the ice dielectric properties, one can expect the bright volcanic regions detected in this study to exhibit a similar range of permittivity. The possibility for igneous material to be that bright is sparsely documented, but the literature suggests that it could be achieved from the combination of both a dense and Ilmenite-rich material (an Iron-Titanium oxide mineral, $FeTiO_3$). Permittivity increases with density, and values of ∼20 have been measured at 4 MHz for dry-volcanic samples from Mount Meager, British Columbia, Canada, with bulk density of 2.4 g/cm³ (Rust et al., 1999). Likewise, Analysis of lunar samples demonstrates that basalt permittivity can strongly increase with Ilmenite content (Chung et al., 1970; Hansen et al., 1973), especially since Ilmenite has a real permittivity ranging from 30 to 80 (Parkhomenko, 1967). Ilmenite-rich terrains have been extensively outlined in volcanic plains on the Moon by both the UV-VIS observations of the Clementine probe (Lucey et al., 2000) and signal absorption reported by the Lunar Radar Sounder (LRS) on the SELENE spacecraft (Pommerol et al., 2010). Yet, an integrative study convolving the positive effect of density and Ilmenite content on the permittivity at MARSIS frequency has yet to be done.

Mouginot et al. (2010) used radar simulations to filter out scattering effects from the surface reflectivity measurements in order to outline first-order permittivity variations at planetary scale. Noteworthily, it can be observed that this inversion also leads to relative permittivity reaching 20 at local scales (Mouginot et al., 2010, Figure 7). Together with our present study, it highlights the potential benefits of considering MARSIS' surface reflectivity for local analyses.

The bright Martian terrains outlined in this study are not a-priori expected to host water-bearing materials at their surface of within their near-surface. They provide well outlined regions with reflection properties similar to the bright polar basal reflector, and they are readily accessible to further remote sensing investigations. Their better characterization would help assessing the likelihood of the various compositional hypotheses for the basal material producing the strong radiometric signatures recorded at the SPLD. The similar geological setting of the detected bright terrains suggest that such set of hypothesis should also consider the possible production of a highly reflective deposit in a volcanic context, possibly through a high density igneous material with metallic inclusions.

Data Availability Statement

The MARSIS Experiment Data Records (EDR) are available through the Geosciences Node of the NASA's Planetary Data System (PDS) archives (https://pds-geosciences.wustl.edu/missions/mars_express/marsis.htm). The relative surface reflectivity $\tilde{R}_{13}$ used in this study have been previously derived from the EDR by Mouginot et al. (2010) and are available on the Texas Data Repository (https://doi.org/10.18738/T8/HMNDH1).

References

Arnold, N. S., Conway, S. J., Butcher, F. E. G., & Balme, M. R. (2019). Modeled subglacial water flow routing supports localized intrusive heating as a possible cause of basal melting of Mars' South polar ice cap. *Journal of Geophysical Research: Planets*, *124*(8), 2101–2116. https://doi.org/10.1029/2019je006061

Bierson, C. J., Tulaczyk, S., Courville, S. W., & Putzig, N. E. (2021). Strong MARSIS Radar reflections from the base of Martian South polar cap may be due to conductive ice or minerals. *Geophysical Research Letters*, *48*(13). https://doi.org/10.1029/2021gl093880

Campbell, M. J., & Ulrichs, J. (1969). Electrical properties of rocks and their significance for lunar radar observations. *Journal of Geophysical Research*, *74*(25), 5867–5881. https://doi.org/10.1029/JB074i025p05867

Cassanelli, J. P., & Head, J. W. (2018). Large-scale lava-ice interactions on Mars: Investigating its role during late Amazonian Central Elysium Planitia volcanism and the formation of Thabasca Alles. *Planetary and Space Science*, *158*, 96–109. https://doi.org/10.1016/j.pss.2018.04.024

Chung, D. H., Westphal, W. B., & Simmons, G. (1970). Dielectric properties of Apollo 11 lunar samples and their comparison with Earth materials. *Journal of Geophysical Research*, *75*(32), 6524–6531. https://doi.org/10.1029/jb075i032p06524

Grima, C., Kofman, W., Herique, A., Orosei, R., & Seu, R. (2012). Quantitative analysis of Mars surface radar reflectivity at 20MHz. *Icarus*, *220*(1), 84–99. https://doi.org/10.1016/j.icarus.2012.04.017

Hansen, W., Sill, W. R., & Ward, S. H. (1973). The dielectric properties of selected basalts. *Geophysics*, *38*(1), 135–139. https://doi.org/10.1190/1.1440325

Khuller, A. R., & Plaut, J. J. (2021). Characteristics of the basal interface of the Martian South polar layered deposits, *Geophysics*, *48*. https://doi.org/10.1029/2021gl093631

Lalich, D. E., Hayes, A. G., & Poggiali, V. (2021). *Explaining bright radar reflections below the martian south polar layered deposits without liquid water*. https://arxiv.org/abs/2107.03497

Lauro, S. E., Mattei, E., Pettinelli, E., Soldovieri, F., Orosei, R., & Cartacci, M. (2010). Permittivity estimation of layers beneath the northern polar layered deposits, Mars. *Geophysical Research Letters*, *37*, 14201. https://doi.org/10.1029/2010GL043015

Lauro, S. E., Pettinelli, E., Caprarelli, G., Guallini, L., Rossi, A. P., & Mattei, E. (2020). Multiple subglacial water bodies below the south pole of Mars unveiled by new MARSIS data. *Nature Astronomy*, *5*, 63–70. https://doi.org/10.1038/s41550-020-1200-6

Looyenga, H. (1965). Dielectric constants of heterogeneous mixtures. *Physica*, *31*, 401–406. https://doi.org/10.1016/0031-8914(65)90045-5

Lucey, P. G., Blewett, D. T., & Jolliff, B. L. (2000). Lunar iron and titanium abundance algorithms based on final processing of Clementine ultra-violet-visible images. *Journal of Geophysical Research*, *105*(E8), 20297–20305. https://doi.org/10.1029/1999je001117

Michalski, J. R., & Bleacher, J. E. (2013). Supervolcanoes within an ancient volcanic province in Arabia Terra, Mars. *Nature*, *502*(7469), 47–52. https://doi.org/10.1038/nature12482

Montési, L. G. J. (2003). Clues to the lithospheric structure of Mars from wrinkle ridge sets and localization instability. *Journal of Geophysical Research*, *108*(E6). https://doi.org/10.1029/2002je001974

Mouginot, J., Kofman, W., Safaeinili, A., Grima, C., Herique, A., & Plaut, J. J. (2009). MARSIS surface reflectivity of the south residual cap of Mars. *Icarus*, *201*, 454–459. https://doi.org/10.1016/j.icarus.2009.01.009

Mouginot, J., Kofman, W., Safaeinili, A., & Herique, A. (2008). Correction of the ionospheric distortion on the MARSIS surface sounding echoes. *Planetary and Space Science*, *56*, 917–926. https://doi.org/10.1016/j.pss.2008.01.010

Mouginot, J., Pommerol, A., Beck, P., Kofman, W., & Clifford, S. M. (2012). Dielectric map of the Martian northern hemisphere and the nature of plain filling materials. *Geophysical Research Letters*, *39*, 2202–n/a. https://doi.org/10.1029/2011GL050286

Mouginot, J., Pommerol, A., Kofman, W., Beck, P., Schmitt, B., Herique, A., et al. (2010). The 3-5 MHz global reflectivity map of Mars by MARSIS/Mars Express: Implications for the current inventory of subsurface H_2O. *Icarus*, *210*(2), 612–625. https://doi.org/10.1016/j.icarus.2010.07.003

Orosei, R., Ding, C., Fa, W., Giannopoulos, A., Hérique, A., Kofman, W. (2020). The global search for liquid after on Mars from Orbit: Current and future perspectives. *Life*, *10*(8), 120. https://doi.org/10.3390/life10080120

Orosei, R., Lauro, S. E., Pettinelli, E., Cicchetti, A., Coradini, M., & Cosciotti, B. (2018). Radar evidence of subglacial liquid water on Mars. *Science*, *361*, 490–493. https://doi.org/10.1126/science.aar7268

Oswald, G., & Gogineni, S. (2008). Recovery of subglacial water extent from Greenland radar survey data. *Journal of Glaciology*, *54*(184), 94–106. https://doi.org/10.3189/002214308784409107

Parkhomenko, E. I. (1967). Dielectric properties of rocks. In G. V. Keller, (Ed.), *Electrical properties of rocks, Monographs in Geoscience*. Springer. https://doi.org/10.1007/978-1-4615-8609-8

Peters, M. E. (2005). Analysis techniques for coherent airborne radar sounding: Application to West Antarctic ice streams. *Journal of Geophysical Research*, *110*(B6), B06303. https://doi.org/10.1029/2004JB003222

Picardi, G., Plaut, J. J., Biccari, D., Bombaci, O., Calabrese, D., & Cartacci, M. (2005). Radar soundings of the subsurface of Mars. *Science*, *310*(5756), 1925–1928. https://doi.org/10.1126/science.1122165

Plaut, J. J., Picardi, G., Safaeinili, A., Ivanov, A. B., Milkovich, S. M., & Cicchetti, A. (2007). Subsurface radar sounding of the south polar layered deposits of Mars. *Science*, *316*(5821), 92–95. https://doi.org/10.1126/science.1139672

Plescia, J. (2000). Geology of the Uranius group volcanic constructs: Uranius Patera, Ceraunius Tholus, and Uranius Tholus. *Icarus*, *143*(2), 376–396. https://doi.org/10.1006/icar.1999.6259

Pommerol, A., Kofman, W., Audouard, J., Grima, C., Beck, P., & Mouginot, J. (2010). Detectability of subsurface interfaces in lunar maria by the LRS/SELENE sounding radar: Influence of mineralogical composition. *Geophysics*, *37*, 3201–n/a. https://doi.org/10.1029/2009GL041681

Rust, A., Russell, J., & Knight, R. (1999). Dielectric constant as a predictor of porosity in dry volcanic rocks. *Journal of Volcanology and Geothermal Research*, *91*(1), 79–96. https://doi.org/10.1016/s0377-0273(99)00055-4

Safaeinili, A., Kofman, W., Mouginot, J., Gim, Y., Herique, A., & Ivanov, A. B. (2007). Estimation of the total electron content of the Martian ionosphere using radar sounder surface echoes. *Geophysical Research Letters*, *34*, 23204–n/a. https://doi.org/10.1029/2007GL032154

Smith, I. B., Lalich, D. E., Rezza, C., Horgan, B. H. N., Whitten, J. L., Nerozzi, S., & Holt, J. W. (2021). A solid interpretation of bright radar reflectors under the Mars South polar ice. *Geophysical Research Letters*, *48*(15). https://doi.org/10.1029/2021gl093618

Sori, M. M., & Bramson, A. M. (2019). Water on Mars, with a grain of salt: Local heat anomalies are required for basal melting of ice at the South Pole today. *Geophysical Research Letters*, *46*(3), 1222–1231. https://doi.org/10.1029/2018gl080985

Telford, W. M., Gedart, L. P., & Sheriff, R. E. (1990). *Applied geophysics* (2nd ed., p. 770). Cambridge University Press.

Tulaczyk, S. M., & Foley, N. T. (2020). The role of electrical conductivity in radar wave reflection from glacier beds. *The Cryosphere*, *14*(12), 4495–4506. https://doi.org/10.5194/tc-14-4495-2020

Whelley, P., Matiella Novak, A., Richardson, J., Bleacher, J., Mach, K., & Smith, R. N. (2021). Stratigraphic evidence for early martian explosive volcanism in Arabia Terra. *Geophysical Research Letters*, *48*(15). https://doi.org/10.1029/2021gl094109

Zuber, M. T., Phillips, R. J., Andrews Hanna, J. C., Asmar, S. W., Konopliv, A. S., & Lemoine, F. G. (2007). Density of Mars' South polar layered deposits. *Science 317*, 1718–1719. https://doi.org/10.1126/science.1146995